Data supplement for Mancini et al., Aberrant Developmental Patterns of Gamma-Band Response and Long-Range Communication Disruption in Youths With 22q11.2 Deletion Syndrome. Am J Psychiatry (doi: 10.1176/appi.ajp.2021.21020190)

EEG Preprocessing

The preprocessing steps were performed by using the free academic software Cartool version 6164 (https://sites.google.com/site/cartoolcommunity/home) as previously described(1,2). In detail, the number of electrodes was reduced from 256 to 204 by eliminating the noisy electrode signals from the cheeks and neck. The data were band-pass filtered between 1 and 140 Hz using non-causal Butterworth filters and we applied additional notch filters at 50, 100 and 150 Hz. The periods of artefacts (e.g., muscle contraction) were marked manually and excluded from further analysis. Noisy channels were identified by means of visual inspection and excluded. The number of accepted epochs did not differ between the two groups [HC: 79.6 ± 11.3; 22q11DS: 76.7 ± 13.13; $t(104)=-1.54$, $p=0.13$]. Independent Component Analysis was used to remove eye-movements (eye blinks and saccades) and ECG artefacts components using a Matlab script based on the EEGlab runica function (https://sccn.ucsd.edu/eeglab/)(3,4). The identified noisy channels were interpolated using a 3D spline interpolation(5). Finally, we applied an instantaneous spatial filter implemented in Cartool that removes local outliers by spatially smoothing the maps without losing its topographical characteristics(6)
and data were recalculated to the common average reference.

Individual Inverse Solution (IS) model

In order to have accurate source estimation and to model reality at best, an individual inverse solution (IS) model was computed for each participant. This is particularly important when investigating a population covering different ages and individuals with 22q11DS who have remarkable volumetric abnormalities of cortical and subcortical brain structures(7–12).

We acquired T1-weighted images with a 3T Siemens Prisma. The parameters for the acquisition of structural images for the T1-weighted MPRAGE sequence in 192 slices with voxel size=0.9x0.9x1.1 mm. T1-weighted images underwent fully automated image processing with FreeSurfer v.6 comprising skull stripping, intensity normalization, reconstruction of the internal and external cortical surface and parcellation of subcortical brain regions. The full head and grey mask files were used for the computation of the individual IS model in Cartool, together with a 3D model of the 204-electrodes cap co-registered with the individual full head. The IS model was computed with 5000 solution points distributed in the grey mask boundaries using Locally Spherical Model with Anatomical Constraints (LSMAC) method for lead field, taking into account the age of the participants to calibrate skull conductivity and thickness (13). The Local Auto Regressive Average (LAURA), a distributed linear source localization method(6,14) was used to determine the IS transformation matrix. Finally, 84 ROIs covering cortical and diencephalon neural structures were extracted from the individual Desikan&Killiany parcellation atlas from Freesurfer computation and used to label the 5000 solution points from the IS model.

Time-Frequency Analyses

Time- frequency analysis (TF) was performed both at scalp level, selecting a cluster of fronto-central electrodes around FCz and in the inverse space.

The preprocessed EEG was down sampled to 500 Hz and exported as epochs of 4 seconds (2 seconds before and after the onset of the stimulus). Time-frequency (TF) decomposition was carried on with in-house Matlab scripts using Morlet transform with full-width at half-maximum (FWHM) on the 4 second epochs. The TF decomposition was performed from 2Hz to 100Hz with a 2Hz step size between frequencies. In order to get rid of the epoch edge artefacts of the TF decomposition, we suppressed the first and last 0.5 seconds of each epoch.

To perform surface analyses, the real and imaginary parts of the TF decomposition were reduced to absolute values equivalent to a frequency power. To perform source analyses, the real and imaginary parts of the TF decomposition were multiplied by the Laura IS transformation matrix (regularisation level of 6) and reduced to absolute value for the 3 directions along x, y and z axes. The obtained 3D vectors were then normalised as the square root of the sum of the squares of the 3 directions in order to get a current density estimation for each solution point equivalent to a frequency power.

For surface and source spaces, the obtained TF signals were averaged across epochs for each participant from – 1.5 to +1.5 seconds relative to the stimulus onset. We then computed event-related spectral perturbations (ERSP) correcting the poststimulus period by the baseline period. The average of the baseline period (defined as the -1.5 to -0.3 seconds interval relative to stimulus onset) was subtracted from and divided by the poststimulus period. We additionally computed for each subject the spectral density as the average of the TF decomposition of all channels and all epochs on the baseline period.

Group Analyses of Time-Frequency Decomposition

We compared gamma-band response between individuals with 22q11DS and controls at surface level and in the inverse space, between deletion carriers with and without psychotic symptoms, between deletion carriers treated and not treated with antipsychotic medications and between deletion carriers with low and high IQ.

At the surface level, first the average spectral density for all channels in the baseline period was compared across groups for each frequency bin. Then, nonparametric Monte-Carlo–based permutations (n=500; 1-100 Hz; 0-1.5 sec, alpha= 0.05, 2-tailed) implemented in Fieldtrip(15) were employed for the statistical testing of group differences in ERSP and ITPC.

At the source space level, after reducing the signal from the individual 5000 solution points to individual 84 ROIs, unpaired t-test were computed between groups of participants. Results were FDR-corrected for the number of ROIs and the number of time-points within a given frequency band selected according to the results at the surface level (i.e., theta: 4-8 Hz and gamma: 38-42 Hz) and in line with previous studies(16). Statistically significant differences in gamma and theta responses are reported in the main text.

Phase-Amplitude Coupling and Group Analyses

We decided to compute the cross-frequency theta-gamma phase-amplitude coupling (PAC) between brain regions showing a task-related increase in gamma for gamma amplitude ROIs and in theta for theta phase ROIs defined as an average increase in gamma power > 15% in the poststimulus period in both the groups of controls and 22q11.2 deletion carriers. PAC is defined as the statistical dependence between the phase of a low frequency such as theta and the amplitude of a higher frequency as gamma(17).

For this analysis, we focused on the first 0.5 sec poststimulus as directed by the theta oscillation differences found only during this period between 22q11.2 deletion carriers and controls during the task. Preprocessed EEG data was filtered into the theta and gamma frequency bands of interest (i.e., 4-8 Hz for theta and 38-42 Hz) and then cut for epochs from – 0.5 to +1.5 seconds. The clean concatenated EEGs filtered for each frequency band were transformed to singular value decomposition (SVD) of each ROIs using an in-house PyCartool toolbox (https://github.com/Functional-Brain-Mapping-Laboratory/PyCartool) with individual IS model and parcellation atlas. The real SVD signals of each ROIs obtained for each frequency bands were computed through Hilbert transform. The instantaneous angles of the SVD for theta frequency band were sorted from complex values. Then, the gamma amplitude envelope of the preselected ROIs was obtained from absolute of complex values of the SVD for gamma

frequency band. Coupling between ROIs was estimated with the modulation index (MI), as described by Tort and colleagues(18) taking into account the 0 to 0.5 sec periods after the onset of stimulus.

In detail, a composite time series was computed as the averaged amplitude of gamma at each binned phase of theta rhythm for each ROI couple. The amplitude distribution was obtained normalizing the mean amplitude by dividing each bin value over the sum of the bins. MI was then defined as the Kullback-Leibler distance of the observed amplitude distribution (P) from the uniform distribution (U) divided by the logarithm of N (i.e., the maximum possible entropy value):

$$MI = \frac{D_{KL}(P, U)}{\log(N)}$$

MI can vary from 0, indicating no relation between theta and gamma, to 1, with gamma amplitude being entirely modulated by theta phase. We estimated the MI for each pair of brain regions in each subject and compared MI values between groups by using paired two-tailed t-tests. Results were finally FDR corrected for multiple comparisons.

Analysis of Confounding Factors

We additionally tested if confounding factors such as the use of antipsychotic medications and the IQ scores influenced ASSR within deletion carriers. Deletion carriers with low IQ were defined as subjects with an IQ lower than the average of the group (i.e., 74) and the remaining deletion carriers were considered as having a high IQ. By employing nonparametric Monte-Carlo–based permutations we did not find any statistically significant difference between deletion carriers treated and not treated with antipsychotic and between deletion carriers with low and high IQ. This last result is in keeping with previous studies not finding a significant effect of IQ on ASSR in individuals with 22q11DS (19).

Auditory Event-Related Potentials

As the early auditory gamma band response (eaGBR) coincides with early evoked potentials such as P50 response, that has been shown to be increased in 22q11DS(20), we carried on ERPs analyses to disentangle the real contribution of gamma response. In detail, we performed a full analysis of the multichannel auditory evoked potential after the onset of the auditory stimulus from 0 to 250 msec with the Cartool software as in previous studies(20). We compared the Global Field Power (GFP), corresponding to the standard deviation of the average referenced potentials of all electrodes, between the two groups for each time point with a randomization test using a significance level of p=0.05. Electric field topography was assessed based on the computation of the Global Dissimilarity (corresponding to the GFP of the difference of the normalized maps) between maps. For statistical analyses, a topographic analysis of variance (TANOVA) was performed; a randomization test based on dissimilarity values by randomly assigning the maps at a given time point to the two groups(21). No statistically significant difference between the groups was observed. Thus, differences observed in specific frequency bands are not entirely attributable to ERPs.

References

1. Cantonas L, Tomescu MI, Biria M, Jan RK, Schneider M, Eliez S, et al. Abnormal development of early auditory processing in 22q11 . 2 Deletion Syndrome. Transl Psychiatry. 2019;15–7.
2. Cantonas L, Mancini V, Rihs TA, Rochas V, Schneider M, Eliez S, et al. Abnormal Auditory Processing and Underlying Structural Changes in 22q11 . 2 Deletion Syndrome. Schizophr Bull. 2020;
3. Makeig S, Jung TP, Bell AJ, Ghahremani D, Sejnowski TJ. Blind separation of auditory event-related brain responses into independent components. Proc Natl Acad Sci U S A. 1997;94(20):10979–84.
4. Jung TP, Makeig S, Westerfield M, Townsend J, Courchesne E, Sejnowski TJ. Removal of eye activity artifacts from visual event-related potentials in normal and clinical subjects. Clin Neurophysiol. 2000;111(10):1745–58.
5. Perrin F, Pernier J, Bertrand O. Spherical splines for scalp potential and current density mapping. Electroencephalogr Clin Neurophysiol. 1989;72:184–7.

6. Michel CM, Brunet D. EEG source imaging: A practical review of the analysis steps. Front Neurol. 2019;10(APR).

7. Schaer M, Debbané M, Bach Cuadra M, Ottet MC, Glaser B, Thiran JP, et al. Deviant trajectories of cortical maturation in 22q11.2 deletion syndrome (22q11DS): A cross-sectional and longitudinal study. Schizophr Res. 2009;115(2–3):182–90.

8. Sun D, Ching CRK, Lin A, Forsyth JK, Kushan L, Vajdi A, et al. Large-scale mapping of cortical alterations in 22q11 . 2 deletion syndrome : Convergence with idiopathic psychosis and effects of deletion size. Mol Psychiatry. 2017;

9. Ching CRK, Ph D, Gutman BA, Ph D, Sun D, Reina JV, et al. Mapping Subcortical Brain Alterations in 22q11 . 2 Deletion Syndrome : Effects of Deletion Size and Convergence With Idiopathic Neuropsychiatric Illness. Am J Psychiatry. 2020;(2):1–13.

10. Mancini V, Sandini C, Padula MC, Zöller D, Schneider M, Schaer M, et al. Positive psychotic symptoms are associated with divergent developmental trajectories of hippocampal volume during late adolescence in patients with 22q11DS. Mol Psychiatry [Internet]. 2020;25(11):2844–59. Available from: http://dx.doi.org/10.1038/s41380-019-0443-z

11. Mancini V, Zöller D, Schneider M, Schaer M, Eliez S. Abnormal Development and Dysconnectivity of Distinct Thalamic Nuclei in Patients With 22q11.2 Deletion Syndrome Experiencing Auditory Hallucinations. Biol Psychiatry Cogn Neurosci Neuroimaging. 2020;5(9):875–90.

12. Bagautdinova J, Zöller D, Schaer M, Padula MC, Mancini V, Schneider M, et al. Altered cortical thickness development in 22q11 . 2 deletion syndrome and association with psychotic symptoms. 2020;1–26.

13. Brunet D, Murray MM, Michel CM. Spatiotemporal analysis of multichannel EEG: CARTOOL. Comput Intell Neurosci. 2011;2011.

14. Grave De Peralta Menendez R, Murray MM, Michel CM, Martuzzi R, Gonzalez Andino SL. Electrical neuroimaging based on biophysical constraints. Neuroimage. 2004;21(2):527–39.

15. Maris E, Oostenveld R. Nonparametric statistical testing of EEG- and MEG-data. J Neurosci Methods. 2007;164(1):177–90.

16. Kirihara K, Rissling AJ, Swerdlow NR, Braff DL, Light GA. Hierarchical Organization of Gamma and Theta Oscillatory Dynamics in Schizophrenia. Biol Psychiatry. 2012;71(10):873–80.

17. Canolty RT, Knight RT. The functional role of cross-frequency coupling. Trends Cogn Sci. 2010;14(11):506–15.

18. Tort ABL, Komorowski R, Eichenbaum H, Kopell N. Measuring phase-amplitude coupling between neuronal oscillations of different frequencies. J Neurophysiol. 2010;104(2):1195–210.

19. Larsen KM, Pellegrino G, Birknow MR, Kjær TN, Baaré WFC, Didriksen M, et al. 22q11.2 Deletion Syndrome Is Associated With Impaired Auditory Steady-State Gamma Response. Schizophr Bull. 2018;44(2):388–97.

20. Rihs TA, Tomescu MI, Britz J, Rochas V, Custo A, Schneider M, et al. Altered auditory processing in frontal and left temporal cortex in 22q11.2 deletion syndrome: A group at high genetic risk for schizophrenia. Psychiatry Res - Neuroimaging. 2013;212(2):141–9.

21. Murray MM, Brunet D, Michel CM. Topographic ERP analyses: A step-by-step tutorial review. Brain Topogr. 2008;20(4):249–64.

FIGURE S1. ASSR paradigm

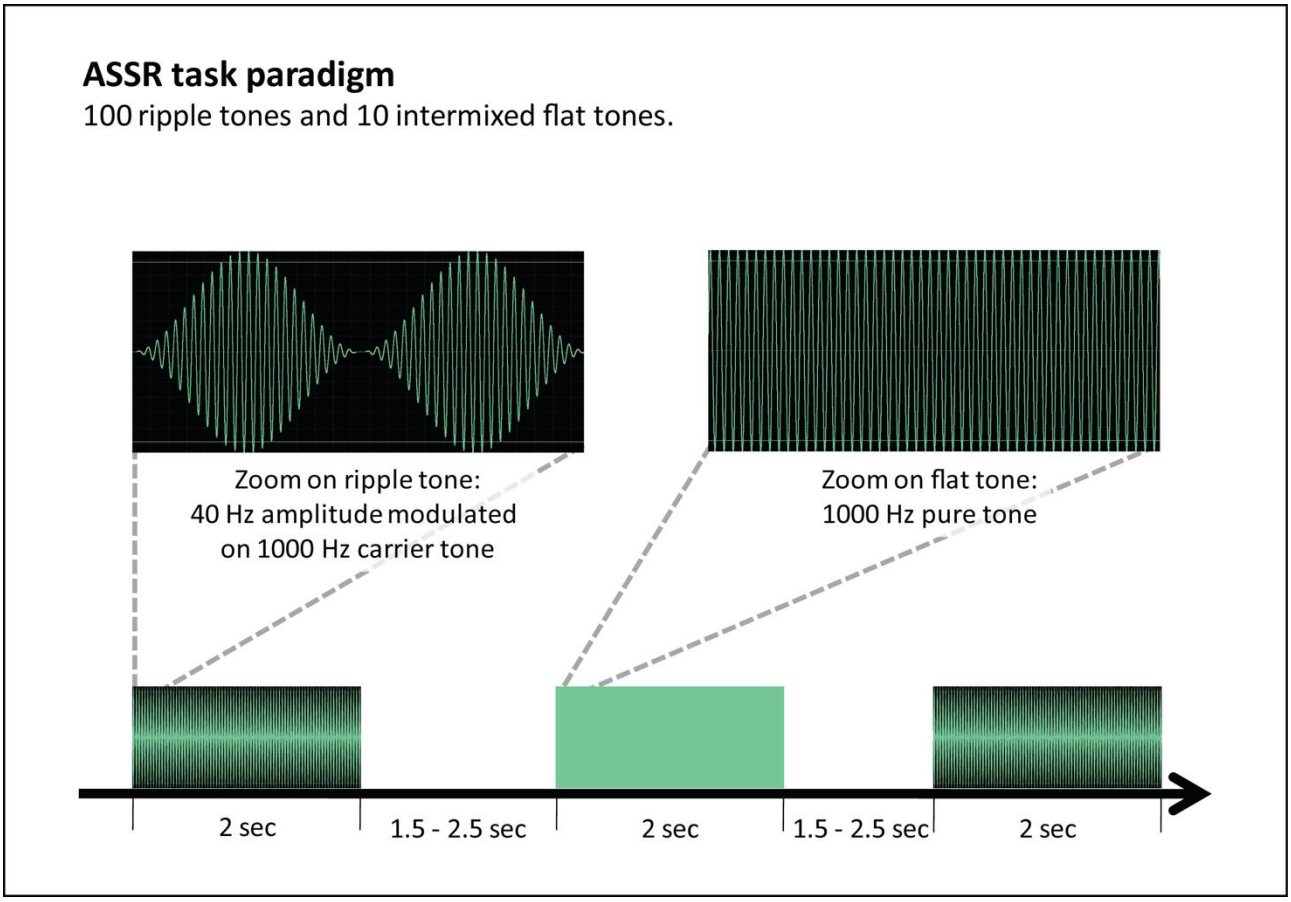

The figure is displaying the ASSR paradigm composed by 100 ripple tones and 10 intermixed flat tones, each lasting 2 seconds. Participants were asked to recognize flat tones only responding by button press.

FIGURE S2. Comparison between controls and non-psychotic deletion carriers

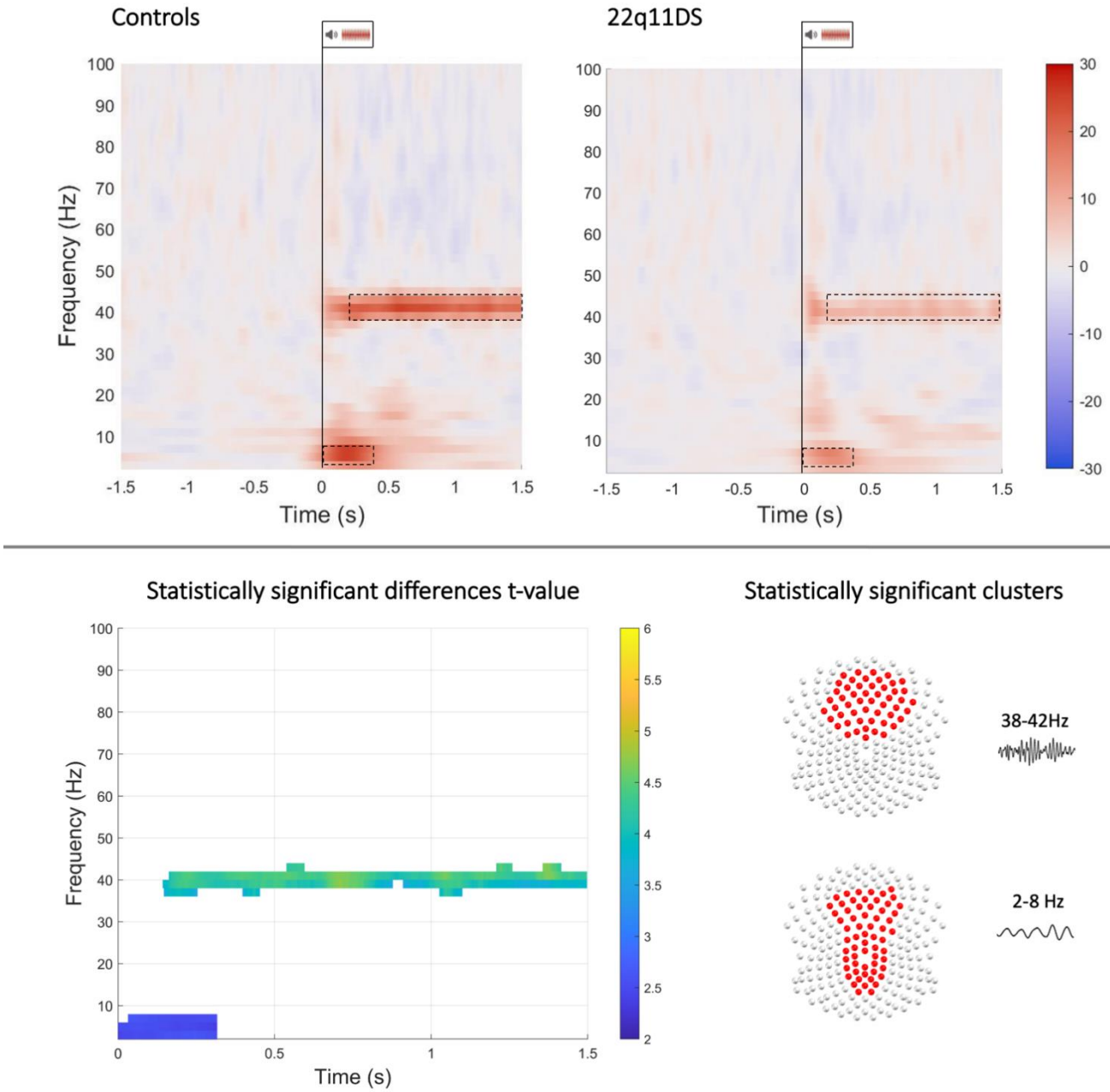

Top panel: time-frequency plots displaying the average pre- and poststimulus event-related spectral perturbation (ERSP) in controls and deletion carriers without psychotic symptoms. The outlined dotted boxes highlight the time-window of statistically significant group differences in gamma and theta power

Bottom panel: significant delta ERSP showing t-values for statistically significant differences in theta and gamma band. Scalp maps display the clusters of electrodes showing statistically significant differences in the gamma and theta bands represented in the time-frequency plots. Power values are expressed in %.

FIGURE S3. ITPC differences between non-psychotic and psychotic deletion carriers

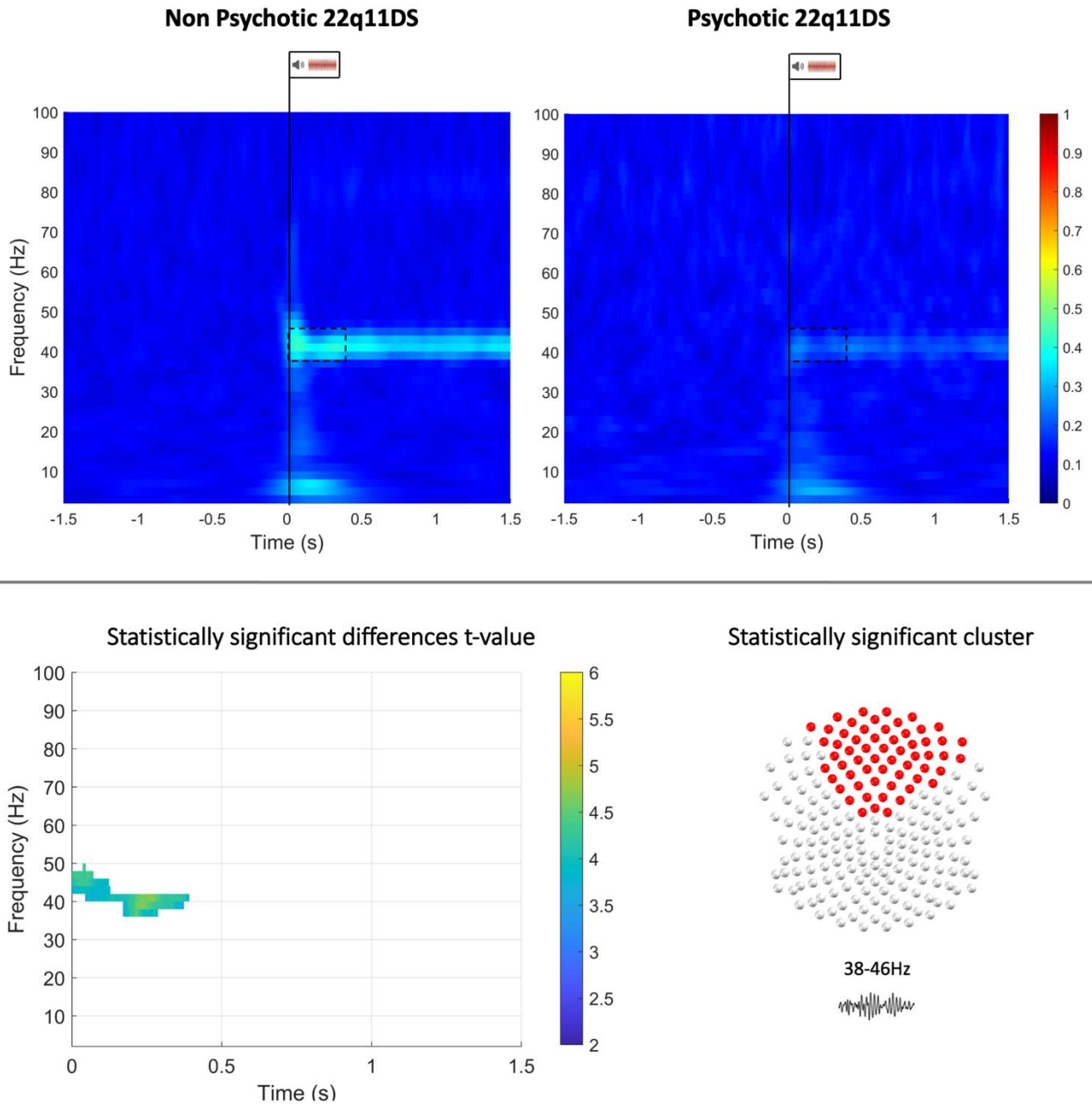

Top panel: time-frequency plots displaying the average pre- and poststimulus inter-trial phase coherence perturbation (ITPC) in non-psychotic and psychotic deletion carriers. The outlined dotted boxes highlight the time-window of statistically significant group differences in gamma and theta power. Bottom panel: on the left t-values for statistically significant differences in theta and gamma band. On the right scalp map displaying the cluster of electrodes showing statistically significant differences in ITPC represented in the time-frequency plot. Power values are expressed in %.